2014 IEEE International Conference on
Automation Science and Engineering (CASE)
Taipei, Taiwan, August 18-22, 2014

A Lightweight Gravity-Balanced Exoskeleton for Home Rehabilitation of Upper Limbs

Hsiang-Chien Hsieh and Chao-Chieh Lan, *Member*, IEEE

***Abstract*—Stroke recovery requires intensive and continuous rehabilitation over a long period of time. Access to existing rehabilitation devices is limited to hospitals due to the considerable cost and maintenance. This paper proposes a lightweight, low-cost gravity-balanced exoskeleton for home rehabilitation of upper limbs. Gravity balancing is based on a two-bar mechanism that can fit the periphery of a human arm. A type of planar flexural spring is proposed to achieve the required spring potential energy. This type of spring has a thin cross-section and can be designed and fabricated conveniently. A model is constructed to optimize the geometry and dimension of the exoskeleton. Performance is evaluated through a static analysis. The results show that the proposed exoskeleton is both simpler and lighter than existing passive devices. It can be easily custom-made for different arm masses and sizes. We expect the exoskeleton to be used in both clinical and homecare environments for the arm rehabilitation of stroke patients.**

***Index Terms*—Gravity balanced exoskeleton, home rehabilitation, upper limb, compliant spring.**

I. Introduction

More than 700,000 people [1] are affected by strokes every year in the US. Strokes, also referred to as cerebrovascular accidents (CVAs), result in a loss of part of the brain function due to a blockage of the blood supply to the brain. Among the various outcomes of a stroke, losing the motor function of the limbs is very common. Stroke rehabilitation is a process designed to enable the stroke sufferer to regain the use of the motor function by means of a physical therapy. To reduce the human labor involved in a manual therapy, robotic therapies have been developed. A robotic therapy usually involves the use of an exoskeleton device whose motion axes and ranges are designed to match with those of a human limb. Patients wear the exoskeleton device to perform training given the support from the device.

Existing arm rehabilitation devices can be classified as either active or passive. An active device usually has several position sensors to identify the human arm motion by detecting the position of the shoulder, elbow, or wrist. After the motion is sensed, the position signal is fed to the computer. Base on this signal, the computer calculates corresponding output force signal to the actuators. Hence the exoskeleton can automatically control its force on the human arm. EXO-UL3 [2] is an active arm rehabilitation robot with seven degrees of freedom (DOFs). Since the robot has the same number of DOFs as the human arm, it has the ability to mimic almost every motion of the human arm. To reduce the moving mass, the electric motor actuation is transmitted using cables and pulleys. ARMin [3] is an active exoskeleton with six DOFs and two rotation actuators. In contrast to EXO-UL3, the actuators in ARMin are attached directly to the exoskeleton at the shoulder and elbow joints, respectively. Except for the arm, active exoskeleton devices for other human joint rehabilitation have been proposed [4~8]. Due to the use of actuators and sensors, active exoskeletons offer more functions and can easily adapt to different patient needs. However, they are typically more expensive and complicated.

The fundamental support from a rehabilitation device is to balance the arm weight so that patients can regain normal arm motion independently. This motivates the development of several passive devices. T-WREX [9, 10] is a passive exoskeleton device comprising several springs and linkages. To reduce the load of the stroke sufferer when performing rehabilitation, T-WREX can compensate the gravity energy of the arm using several springs. Due to the adjustable length and strength of the springs and linkages, the device can be easily tailored to patients of different arm sizes. NeReBot [11] is a kind of passive arm rehabilitation device. Unlike an exoskeleton device, NeReBot lifts the human arm up with several slings to make patients move their arm easily to satisfy the rehabilitation purpose. Without the hand-motored function, NeReBot has a limited operation range. Nevertheless, many hospitals still choose to use NeReBot owing to its simple structure, low cost and ease of operation. In general, passive devices have no power input or electric components, and are therefore simple, reliable and economic. As a result, they are commonly preferred over active devices for practical applications despite their lower adaptivity.

An effective stroke recovery relies upon intensive and continuous rehabilitation over a long period of time. Access to existing active or passive rehabilitation devices is limited to hospitals due to their high cost, bulky size, complexity, and maintenance issues. Since the rehabilitation activities must be conducted in hospitals, patients will suffer from a longer period of recovery time if they have less readily access to hospitals. It has been shown [12, 13] that home rehabilitation can be equivalently effective as hospital rehabilitation. Home environment is friendlier and can reduce the demand on hospital resources. To support widespread deployment in homecare environments, there is a need for portable, light, and affordable rehabilitation devices.

Considering the challenges of effective and economic rehabilitation, this paper proposes a passive rehabilitation device that is tailor-made for each patient. We focus here on a device to support the weight of a human upper limb, since this

This work was supported in part by the by the Ministry of Education, Taiwan, R.O.C. under the NCKU Project of Promoting Academic Excellence and Developing World Class Research Centers. H.-C. Hsieh and C.-C. Lan are with the Department of Mechanical Engineering, National Cheng Kung University, No. 1, University Rd., Tainan, Taiwan. (Corresponding author e-mail: cclan@mail.ncku.edu.tw).

978-1-4799-5283-0/14/$31.00 ©2014 IEEE

is the most important function of the rehabilitation device. A special type of compliant spring is designed to meet the weight requirement of each individual. The avoidance of adjustment and power input makes the device much simpler. The lightweight and low-cost device is affordable to every patient so that rehabilitation can be realized at home.

The remainder of this paper is organized as follows. Sec. II presents the design of the gravity-balanced upper limb exoskeleton. The design and analysis of the flexural springs are given in Sec. III. Sec. IV verifies the performance of the exoskeleton by computer simulation. Finally, Sec. V presents the concluding remarks.

II. The Proposed Gravity- Balanced Exoskeleton

2.1 Challenges of Existing Gravity Balancing Approaches

There are several types of mechanisms that can be applied to construct a gravity-balanced rehabilitation device. The mechanism used in the popular T-WREX [9, 10] is shown in Fig. 1. The weight balance of an upper arm is achieved by using a parallel four-bar mechanism with a connecting spring. The points denoted as m_1 and m_3 represent the centers of mass of the two side link, while the point denoted as m_2 represents the center of mass of the upper limb. Given the position vectors $\mathbf{a}_1$, $\mathbf{b}_1$, $\mathbf{s}_1$~$\mathbf{s}_3$, $\mathbf{r}_1$ and masses m_1~m_3, the spring stiffness K can be obtained as follows.

$$K = \frac{(m_1|\mathbf{s}_1| + m_2|\mathbf{r}_1| + m_3|\mathbf{r}_1| + m_3|\mathbf{s}_3|)|\mathbf{g}|}{|\mathbf{a}_1||\mathbf{b}_1|} \quad (1a)$$

$$\lambda_1 = \pi - \theta_1 \quad (1b)$$

In addition to the stiffness K, the spring must also have a pretension to balance with the arm weight. Although the parallel four-bar has been successfully realized, it is relatively more complicated because of more components. An exoskeleton based on the parallel four-bar cannot easily fit the periphery of an upper arm. There will be unavoidable extruded portion that limits the motion and hence is less portable.

Fig. 2 shows the proposed two-bar mechanism as an alternative for gravity balancing. This mechanism has a much simpler geometry. There is only one moving link with one connecting spring. The mass m_1 includes those from the link and the arm. Its position is described by vector $\mathbf{s}_1$. Similar to that in Eq. (1), the spring stiffness can be obtained as follows.

$$K = \frac{m_1|\mathbf{g}||\mathbf{s}_1|}{|\mathbf{a}_1||\mathbf{b}_1|}, \quad (2a)$$

$$\lambda_1 = \pm(\pi - \theta_1) \quad (2b)$$

Given the proper stiffness of the spring, the two-bar mechanism can balance the weight of the arm in the same way as the parallel four-bar mechanism. Without compromising structural rigidity, an exoskeleton made by using the two-bar mechanism is expected to have a simpler structure.

The spring for the mechanism in Fig. 1 needs to have a very specific stiffness in order to balance the weight. The helical springs shown in Fig. 3(a) have been commonly used in a gravity-balanced mechanism as the energy storage component. In this paper, we proposed a planar flexural spring shown in Fig. 3(b) to serve as the energy storage component. The flexural spring has several merits that make it more suitable for use in a gravity-balanced exoskeleton.

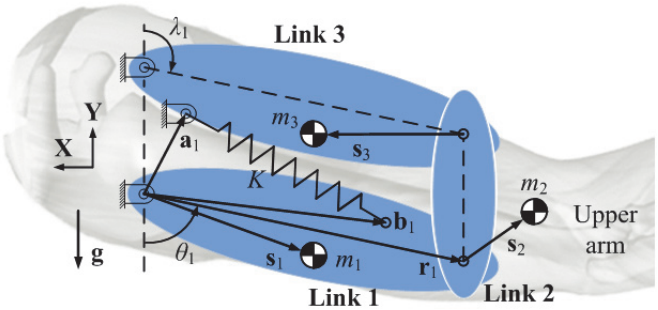

Fig. 1 A parallel four-bar mechanism for gravity balancing

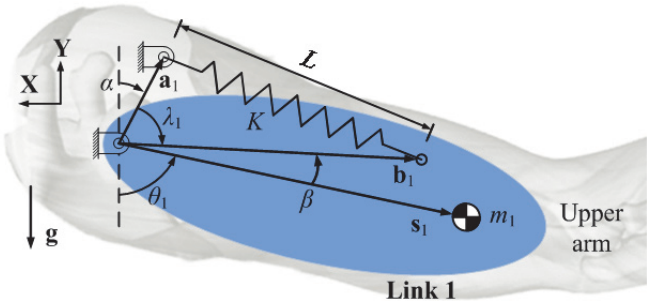

Fig. 2 A two-bar mechanism for gravity balancing

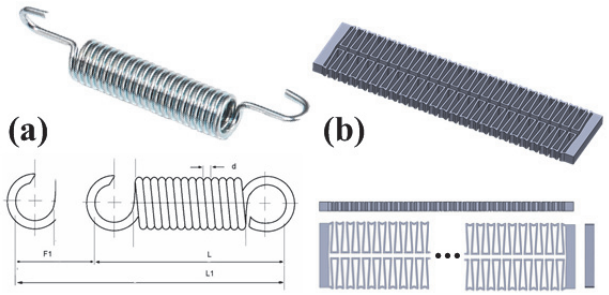

Fig. 3 (a) Helical spring (b) The proposed planar flexural spring

i. Helical springs are made of specialized wire wrapping machines. The stiffness of a helical spring depends on the wire and coil diameters, which usually have a finite number of combinations. Specifying an arbitrary stiffness would be costly because it would require extra demand on the wrapping machine and wire dimension. The proposed planar flexural spring can be fabricated by common CNC machines or 3D printers. The stiffness can be adjusted to any value by changing the in-plane thickness, without affecting the volume of the spring.
ii. The flexural springs are made of polymer materials. Compared with spring steel, polymer is lighter and hence can reduce the load on a human body.
iii. Unlike helical springs that have a cylindrical shape, the flexural spring has a thin cross-section. When multiple flexural springs are used, they can be arranged to fit the periphery of a human arm. The device can then be streamlined.

2.2 Design and Analysis of the Two-bar Balancing Mechanism

Fig. 4 shows the CAD model of the proposed arm rehabilitation device, which is based on the two-bar mechanism shown in Fig. 2. The device has a light weight and can be easily worn by a patient. The multiple tension springs employ the design in Fig. 3(b) and can fit the upper arm smoothly. Fig. 5 shows the motion snapshot of the device. The

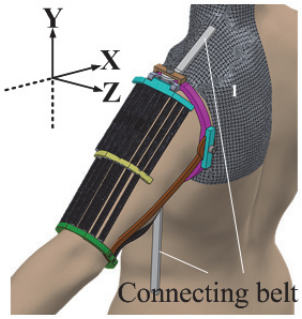

Fig. 4 CAD model of the exoskeleton device

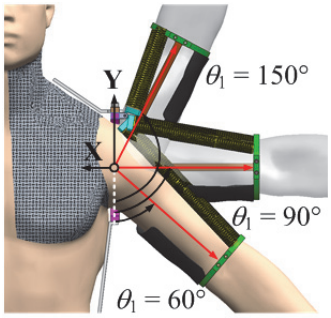

Fig. 5 Motion snapshot of the rehabilitation device

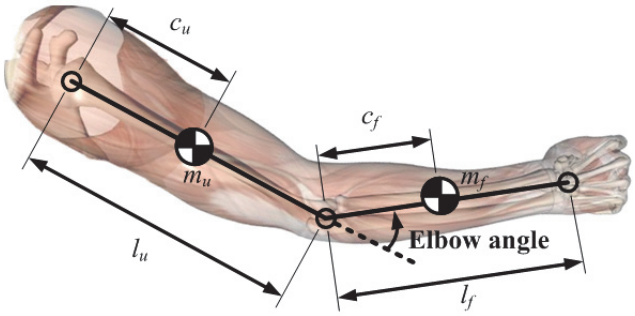

Fig. 6 Parameters of a human upper limb

device is attached to the trunk by using two connecting belts. The proposed device is shown to be much smaller than existing rehabilitation devices. Patients are allowed to move their arm more freely from θ_1 of 0° to 180°. The tension springs covering the skin will provide enough force to support the weight of the human arm.

Since the rotation of the shoulder is much larger than the rotation of the elbow, we consider a case where the movement of the arm only includes the rotation of the shoulder. The rotation of the elbow joint is ignored since its effect on the position of the mass center of the arm is limited. Considering this, the whole arm can be treated as if the elbow is fixed at a certain angle and the position of the mass center of the whole arm will not change.

To design and analyze the balancing mechanism, the energy functions must be derived. With reference to [14], the potential energy due to gravity can be represented as

$$E_g = -m_1|\mathbf{g}||\mathbf{s_1}|\cos\theta_1 = -m_1\mathbf{g}\cdot\mathbf{s_1} \tag{3}$$

The spring length L can be expressed as

$$L = |\mathbf{b_1} - \mathbf{a_1}| \tag{4}$$

Thus, the potential energy due to spring deformation is

$$E_s = \tfrac{1}{2}K(L - L_0)^2 \tag{5}$$

Assuming that a zero free-length spring was used ($L_0 = 0$), Eq. (5) can be rewritten as

$$\begin{aligned} E_s &= \tfrac{1}{2}KL^2 = K_1(\mathbf{a}_1\cdot\mathbf{b}_1) + \tfrac{1}{2}K(\mathbf{a}_1\cdot\mathbf{a}_1 + \mathbf{b}_1\cdot\mathbf{b}_1) \\ &= K(\mathbf{a}_1\cdot\mathbf{b}_1) + \tfrac{1}{2}K(|\mathbf{a}_1|^2 + |\mathbf{b}_1|^2) \end{aligned} \tag{6}$$

The total potential energy includes those from gravity and the spring deformation.

$$E_t = \left[-m_1\mathbf{g}\cdot\mathbf{s}_1 + K(\mathbf{a}_1\cdot\mathbf{b}_1)\right] + \tfrac{1}{2}K(|\mathbf{a}_1|^2 + |\mathbf{b}_1|^2) \tag{7}$$

To reach a state of static balance so that the upper limb does not have to exert any force, the total energy has to be constant for every θ_1. Since both $|\mathbf{a}_1|$ and $|\mathbf{b}_1|$ are constant, setting the first term of the right hand of Eq. (7) as zero would result in a constant E_t. This leads to the expression in Eq. (2) which can be used to calculate the proper spring stiffness.

To obtain the values of m_1 and $\mathbf{s}_1$, the mass property of the upper limb must be given. Fig. 6 shows the diagram that defines the parameters of a human upper limb. Without loss of generality, we consider here a set of parameters listed in Table 1. Since the elbow angle may range from 0° to 90°, which will change the position vector $\mathbf{s}_1$, the average 45° was used to minimize the difference of mass center position caused by elbow angle. In the 45° case, it can be shown that m_1 is 3.36 kg

Table 1 Parameters of a human upper limb

Upper arm	Forearm
m_u = 1.8425 kg	m_f = 1.5136 kg
l_u = 305.2 mm	l_f = 283.8 mm
c_u = 152.6 mm	c_f = 142.1 mm

Table 2 Parameters of the two-bar mechanism

m_1 = 3.36 kg, $\|\mathbf{s}_1\|$ = 266.8 mm, $\|\mathbf{a}_1\|$ = 82.5 mm, $\|\mathbf{b}_1\|$ = 250 mm, α = 10°, β = 12°

and $|\mathbf{s}_1|$ is 266.8 mm. Other parameters for the two-bar mechanism are listed in Table 2.

Based on Eqs. (3~7) and the parameters in Table 2, a simulation has been performed with results shown in Fig. 7(a). The calculated stiffness is K = 0.43 N/mm. We focus on an operation range defined from θ_1 of 30° to 120°. In this range, the total energy E_t slightly varies from 11.41 J to 12.56 J. The average energy is 11.75 J. The E_t curve shows that the mechanism satisfies the balance condition. To make the E_t curve constant, the angles α and β have to be zero. However, α and β can only achieve small values (10° and 12° given in Table 2) and cannot be zero because the device would then interfere with the human arm.

The results in Fig. 7(a) were obtained assuming that spring has a zero free length. In practice, the nonzero free length of the spring must be accounted for. As shown in Fig. 7(a), the spring energy decreases as θ_1 increases. Hence the spring length will decrease with increasing θ_1. We consider here a case where the spring will decrease to its free length at θ_1 = 160°. At this angle, we set the free length to be 150 mm. Thus θ_1 of 160° becomes the limit of rotation. Another simulation was performed after including the effect of the free length. The results are shown in Fig. 7(b). The total energy increases from −2.31 J to 4.76 J in the operation range. The obvious increase indicates that the weight is not balanced.

Considering the effect of the spring free length, the spring stiffness must be recalculated to restore balance. Since Eq. (2) is only valid for zero free length, we seek a numerical solution through the optimization toolbox in MATLAB. Table 3 lists the optimization formulation. Given the design parameters, the objective is to find a value of K such that the flatness in the operation range is minimized, where flatness is defined as the difference of maximum and minimum E_t, divided by the average E_t. The constraint is that the elongated length ΔL cannot be larger than the free length of the spring. The result of the optimization is K = 1.00 N/mm. The elongation ΔL of the spring is 150 mm when θ_1 = 0°. The energy diagram is

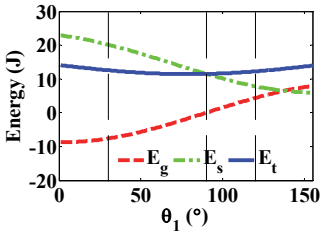

Fig. 7(a) Energy diagram of zero spring free length L_0

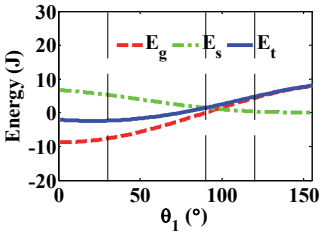

Fig. 7(b) Energy diagram of nonzero spring free length (L_0 = 150 mm)

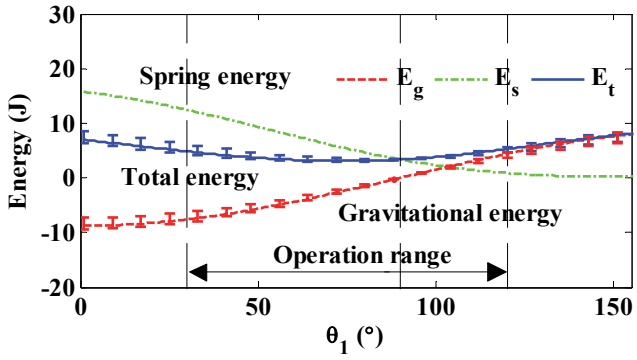

Fig. 7(c) Energy diagram after optimization

Table 3 Formulation of stiffness optimization

1. *Objective*: Given m_1,$\|\mathbf{s}_1\|$, $\|\mathbf{a}_1\|$,$\|\mathbf{b}_1\|$, and L_0, minimize the flatness in the operating range where flatness is defined as $(E_{t,\max} - E_{t,\min}) / E_{t,\text{ave}}$ in the operation range
2. *Design variable: K*
3. *Constraint:* $\Delta L/L_0 < 100\%$

shown in Fig. 7(c). The maximum and minimum E_t are 5.27 J and 3.08 J, respectively. Compared with that in Fig. 7(b), the variation of total energy has been reduced. To further reduce energy variation without introducing other linkages, the angles α and β must approach zero.

The error bars of the gravity energy and total energy curves in Fig. 7(c) are used to indicate the energy variation due to an elbow angle between 0° and 90°. As can be seen, the variation is small compared with the variation of the curves themselves. This verifies our previous assumption of using elbow angle of 45° to obtain $|\mathbf{s}_1|$. The variation is the smallest in the neighborhood of θ_1 = 90°, which is the region with most frequent arm motion.

2.3 Mechanical Design

Using the optimized parameters in Sec. 2.2, we further build a CAD model of the rehabilitation device. As Fig. 8 shows, the device is designed to be worn on the left arm. It comprises six components. Component 1 (shown in Fig. 4) is rigidly connected to the human body. Component 2 is connected to 1 through a revolute joint. The rotation of component 2 about 1 is denoted as the pitch motion. The yaw motion denotes components 3 and 4 of rotating θ_1 about component 2. Components 3 and 4 are fixed together to hold the arm and move with the upper arm. Component 5 and the flexural springs connect components 2 and 4. This device has two DOFs with dimension of 170×170×310 mm^3. Since the device has a simple structure and minimal number of components, it can be easily fabricated and assembled. The

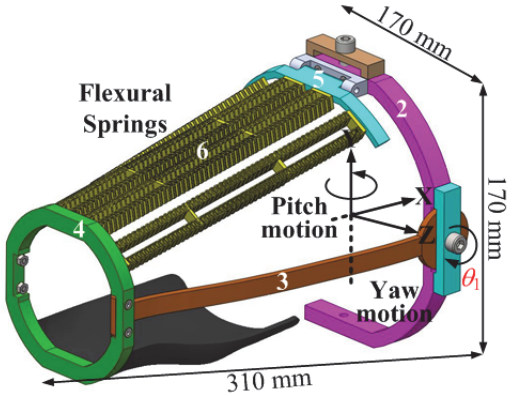

Fig. 8 Detailed view of the rehabilitation device

device can be custom-made to fit each individual's arm size with minimum extruded portion.

III. Design of the Flexural Springs

3.1 Spring Arrangements

Although only one spring is needed for the device, it would be better to use multiple springs whose equivalent stiffness is the same as that of using one spring. Using multiple springs can reduce the size of the spring and distribute the load. Three different arrangements are considered, as shown in Fig. 9. In Case 1, four identical springs of stiffness k are used. They are placed parallel to each other. In Case 2, eight springs are used. They are divided into two groups; one has three identical springs and the other has five identical springs. Similarly, Case 3 has 16 springs that are divided into seven and nine. The equivalent stiffness K is obtained from the following.

$$1/K = 1/n_1k + 1/n_2k \tag{8}$$

where n_1 and n_2 are the numbers of springs of the first and second groups, respectively. The value of k for each spring can be obtained from the optimization formulation introduced in Sec. 3.2. To achieve the overall free length L_0 = 150 mm and an elongation proportional to the free length, the lengths of the springs must satisfy

$$x + y = 150,\ n_1kx = n_2ky \tag{9a, b}$$

where x and y are the spring free lengths in the first and second groups, respectively. Using Eqs. (8~9), the spring parameters can be obtained. Table 4 lists the detailed results. As can be seen, the stiffness of Case 2 is almost twice the stiffness of Case 1, primarily because the springs are shorter. Case 3 has more springs and hence its stiffness is comparable to that of Case 1. While all the three cases are possible, we use Case 1 in this study for the arrangement of the springs. It has fewer springs than the other two.

3.2 Shape and Dimension Design of the Flexural Spring

The flexural spring in Fig. 3(b) must satisfy a specified stiffness. This section proposes a formulation to design the flexural spring to meet the stiffness requirement. Fig. 10(a) shows the schematic of the design model. The flexural spring comprises N identical cells that are serially connected. Each cell is symmetric with width $2L_x$ and height L_y. The design of the whole spring can be simplified to the design of a single cell. Fig. 10(b) shows the design model of the cell. Due to symmetry, only one half of the cell is considered. For a given size and material, the stiffness of the cell depends on its shape,

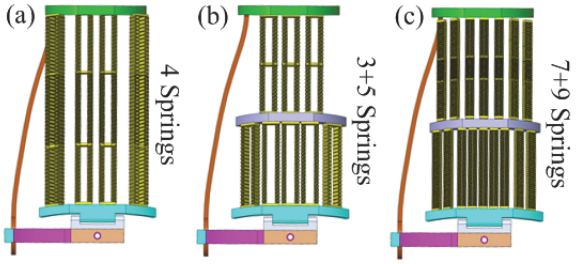

Fig. 9 Different spring arrangements: (a) Case 1 (b) Case 2 (c) Case 3

Table 4 Parameters of the flexural springs

	Case 1	Case 2		Case 3	
Stiffness k (N/mm)	0.250	0.533		0.254	
Number of springs	4	$n_1 = 3$	$n_2 = 5$	$n_1 = 7$	$n_2 = 9$
Free length (mm)	150	94	56	85	65
Out-of-plane thickness (mm)	10	10		5	

in-plane thickness w, and out-of-plane thickness t. As shown in Fig. 10(b), the shape includes five straight segments with six controlling nodes $\mathbf{n}_1$~$\mathbf{n}_6$. Hence the shape further depends on the node positions. An optimization algorithm can be implemented to find the optimal combination of shape and thicknesses to achieve the desired stiffness. The constraints would be the stress, interference, and machinable size. Detailed optimization formulation can be found in [15].

3.3 *Simulation and Verification*

Using Case 1 in Fig. 9(a) as the spring arrangement, the stiffness of each spring has to be 0.25 N/mm. An optimization based on the design model in Sec. 3.2 has been performed. Polyaryletherketone (PEEK) was used as the material. The detailed optimized parameters are listed in Table 5. The spring has a dimension of 150×33×10 mm^3.

A finite element analysis has been performed to compute the stiffness of the spring. Fig. 11 shows the force to displacement curve of the spring. The FEA curve has a stiffness of 0.2498 N/mm, which is very close to the desired 0.25 N/mm. At ΔL = 150 mm, the maximal stress is 85.80 MPa, which is well below the yielding stress of the material. To further verify the numerical results, a prototype is fabricated by using a CNC machine. Fig. 12 shows the fabricated spring. We further conduct an experiment to measure its actual stiffness. The experimental F-ΔL curve is shown in Fig. 11. The experimental stiffness is 0.276 N/mm, which is slightly higher than the simulation one. The small discrepancy is a result of unavoidable machining error.

Since the springs need to adapt to different loads, their stiffness must be able to change conveniently without the need to perform another optimization. This can be accomplished by changing the in-plane thickness w or out-of-plane thickness t based on the following relationship.

$$k \propto tw^3 \tag{10}$$

If a stiffness of 0.3 N/mm is required, then t should be increased to 15 mm or w should be increased to 0.991 mm.

IV. Static Analysis of the Rehabilitation Device

The previous energy curve in Fig. 7(c) was obtained by using the analytical equations in Sec. 2.2. A numerical static

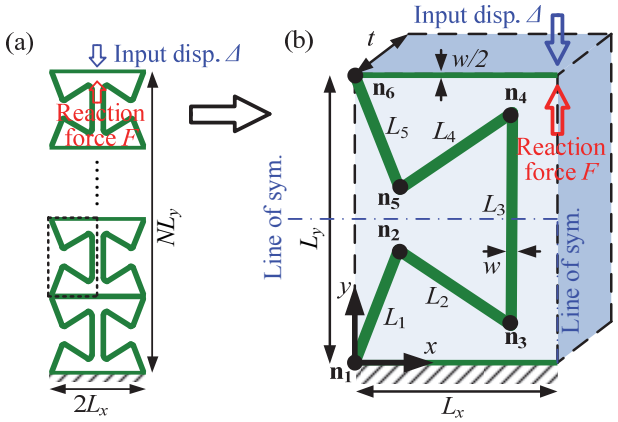

Fig. 10 Schematic of the flexural spring design model

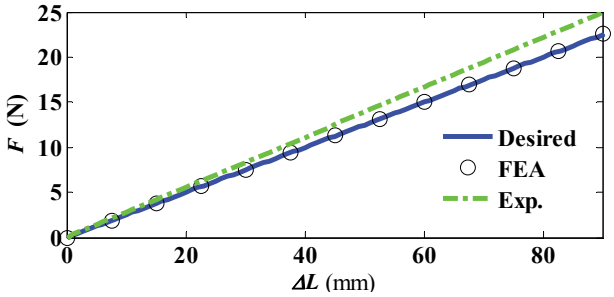

Fig. 11 Force-to-displacement curve of the spring

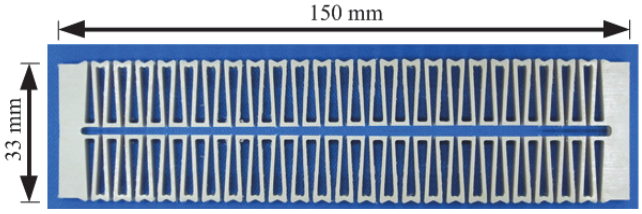

Fig. 12 Flexural spring prototype

Table 5 Optimized parameters of the flexural spring

L_x = 20 mm, L_y = 5.42 mm, N = 24,
Out-of-plane thick. t = 10 mm, in-plane thick. w = 0.866 mm
Elastic modulus E = 3.588 GPa, yield stress σ_y = 210 MPa
Stiffness k = 0.2498 N/mm, maximum stress = 85.80 MPa

analysis (implemented in ANSYS) has been performed using the solid model in Fig. 8 to verify the actual balancing performance of the two-bar mechanism. Fig. 13(a) shows the model constructed in ANSYS. Four linear springs of stiffness 0.25 N/mm are used to represent the flexural spring shown in Fig. 11. Fig. 13(b) shows three different positions of the rehabilitation device. The total spring energy was obtained for θ_1 = 0°~140°. Fig. 14 shows the result. As can be seen, the numerical curve is slightly higher than the analytical one. This is because in the analytical model the geometry of component 5 is not considered. Since the two ends of each spring are required to connect to a revolute joint, component 5 serves as the common revolute joint for the four springs to avoid making the device too complicated. To obtain a spring energy curve same as the analytical one, the stiffness must be made smaller. A spring energy curve with k of 0.215 N/mm was obtained and shown in Fig. 14. It almost matches with the analytical one. This spring energy curve can then be used to balance with the gravity energy curve.

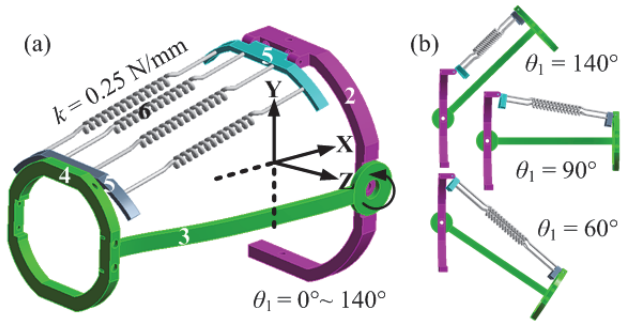

Fig. 13 Static simulation using ANSYS

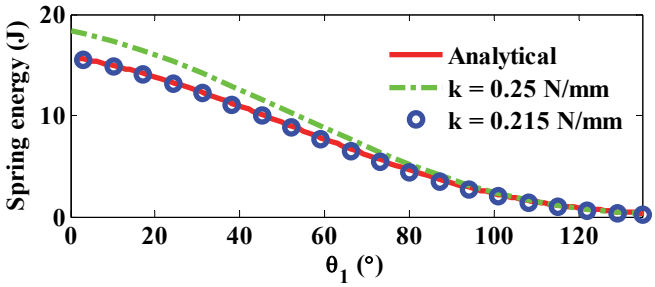

Fig. 14 Potential energy due to spring

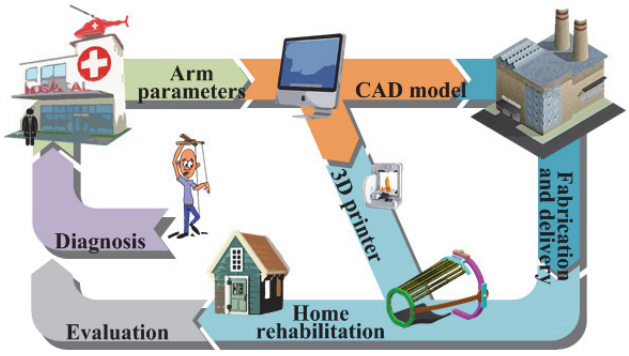

Fig. 15 Illustration of home rehabilitation

V. Discussion and Conclusion

This paper has presented the design and analysis of an exoskeleton for home rehabilitation of injured human arms. By using the proposed balancing mechanism and flexural springs, the exoskeleton has been shown to hold the following novelties.

1. Unlike other passive exoskeletons, this device has minimum number of components. Its geometry fits the periphery of a human arm. Wearing the device is very much like wearing a sleeve. It can also be custom made for each specific arm.
2. The device is portable and readily used at home. Each individual component can be fabricated by using standard CNC machines or 3D printers.

Fig. 15 shows the flowchart to achieve home rehabilitation. The patient is first diagnosed by doctors in a hospital. The arm parameters of the specific patient is then measured and used to generate the CAD model of the device custom-made for the patient. The device can then be fabricated in a machine shop and then delivered to the patient at home. With the wide availability of 3D printers, the device may even be printed at home and then assembled. The patient then follows the instructions to rehabilitate the injured arm. Since the device has a simple structure, maintenance and repair can be easily achieved at home. After a period of time, the patient then visits the hospital for evaluation of the arm. This procedure minimizes the visits to the hospital and can facilitate the rehabilitation activity for those who cannot visit the hospital too often.

The exoskeleton has been preliminarily verified by means of ANSYS simulation and experiment. In our future studies, an exoskeleton prototype will be fabricated and its performance will be evaluated experimentally and clinically. We expect this type of gravity-balanced exoskeleton to be used in combination with active rehabilitation devices to reduce the required capacity of actuators.

References

[1] R. Wayne et al., 2007, “Heart disease and stroke statistics – 2007 update. A report from the American heart association statistics committee and stroke statistics subcommittee,” Circulation published by the American Heart Association 2006. 7272 Greenville Avenue, Dallas, Texas.

[2] J.C. Perry, J. Rosen, and S. Burns, 2007, “Upper-limb powered exoskeleton design,” IEEE/ASME Transactions on Mechatronics, 14(4), pp. 408-417.

[3] T. Nef, M. Mihelj, G. Kiefer, C. Perndl, R. Müller, 2007, “ARMinexoskeleton for arm therapy in stroke patients,” Rehabilitation Robotics, pp. 68-74.

[4] S. Balasubramanian et al., 2008, “Rupert: an exoskeleton robot for assisting rehabilitation of arm functions,” Virtual rehabilitation, IWVR, pp. 163-167.

[5] N. Vitiello et al., 2013, “NEUROExos: a powered elbow exoskeleton for physical rehabilitation,” IEEE Transactions on Robotics, 29(1), pp. 220-235.

[6] S. K. Agrawal et al., 2007, “Assessment of motion of a swing leg and gait rehabilitation with a gravity balancing exoskeleton,” IEEE Transactions on Neural Systems and Rehabilitation Engineering, 15(3), pp. 410-420.

[7] B. Weinberg et al., 2007, “Design, control and human testing of an active knee rehabilitation orthotic device,” IEEE Int. Conf. on Robotics and Automation, pp. 4126-4133.

[8] A. Gupta et al., 2008, “Design, control and performance of RiceWrist: A force feedback wrist exoskeleton for rehabilitation and training,” The International Journal of Robotics Research, 27(2), pp. 233-251.

[9] R. J. Sanchez et al., 2006, “Automating arm movement training following severe stroke: functional exercises with quantitative feedback in a gravity-reduced environment,” IEEE Trans Neural Systems and Rehabilitation Engineering, pp. 378-389.

[10] D. Gijbels et al., 2011, “The Armeo spring as training tool to improve upper limb functionality in multiple sclerosis: a pilot study,” Journal of Neuroengineering and Rehabilitation, 8(5), 5.

[11] S. Masiero, A. Celia, M. Armani, and G. Rosati, 2006, "A Novel Robot Device in Rehabilitation of Post-stroke Hemiplegic Upper Limbs," Aging Clinical Experimental Research, pp. 531-535.

[12] M. Britton and A. Andersson, 2000, “Home rehabilitation after strok,” International Journal of Technology Assessment in Health Care, 16(03), pp. 842-848.

[13] C. Anderson et al., 2000, “Home or hospital for stroke rehabilitation? Results of a randomized controlled trial I: Health outcomes at 6 months,” Stroke, 31(5), pp. 1024-1031.

[14] W.-B. Shieh, D.-Z. Chen, and P. Y. Lin, 2007, “Design of statically balanced planar four-bar linkages with base-attached springs,” in 12th IFToMM World Congress, Besançon, France, pp. 18-21.

[15] C.-C. Lan and Y.-J. Cheng, 2008, “Distributed shape optimization of compliant mechanisms using intrinsic functions,” Journal of Mechanical Design, 130, 072304.